Effect of the thickness of diamond-like carbon layer on local temperature increase on multi-layered structure induced by laser heating

Peng Yu, Weidong Zhou, Shengkai Yu*

*Data Storage Institute, Agency for Science, Technology and Research (A*STAR), DSI Building, 5 Engineering Drive 1, Singapore 117608*

* Corresponding Author:

Peng Yu

DSI Building, 5 Engineering Drive 1, Singapore 117608

Tel: 65-6874-8623

Fax: 65-6516-0900

Email: yu_peng@dsi.a-star.edu.sg

Running title: Effect of diamond-like carbon layer on local temperature increase

Effect of the thickness of diamond-like carbon layer on local temperature increase on multi-layered structure induced by laser heating

The present study concerns the effect of the thickness of overcoating layer on local temperature increase in the multi-layered structure subject to laser heating. The numerical simulation indicates that the presence of the diamond-like carbon (DLC) layer on the top of multi-layered structure enhances local temperature increase, compared with the same structure without the DLC layer. This enhancement gradually becomes significant with an increase in the thickness of DLC layer. The DLC layer only absorbs small amount of laser energy. However, the energy accumulates in the DLC layer due to its low thermal conductivity, resulting in significant temperature increase.

Keywords: laser heating, multi-layered structure, diamond-like carbon

Introduction

Diamond-like carbon (DLC) is an amorphous carbon with a high fraction of diamond-like (sp^3) bonds. The properties of DLC range between those of diamond and graphite. The properties of DLC such as density ρ, heat capacity C_p and thermal conductivity κ can be tuned by changing the sp^3 content, the organization of the sp^2 sites, and the hydrogen or nitrogen content [1-3]. Moreover, DLC can be deposited at room temperature. These advantages make DLC a promising material as a protective coating. For example, the ultrathin DLC films have been applied to high-density data storage in magnetic and optical disks [1]. The DLC overcoating film is also widely applied in microsystem in biomedical and biological applications [4].

In many situations, the DLC film may suffer harsh environment such as high temperature and thermal stress. For example, in heat-assisted magnetic recording (HAMR), the FePt recording layer has to be heated above its Curie temperature (700K) during the writing cycle [5]. This is accomplished with a laser beam imposed on a small region of the disk surface. The temperature field on the disk thus becomes highly non-uniform around the region heated by the laser beam. The thermal stability of the DLC overcoating film above the FePt layer thus attracts great concern. In another application, the DLC film is utilized as a heat source to accelerate crystallization of silicon films by laser irradiation with a low energy density [6], which benefits from the high optical absorbance and the high heat resistance of DLC film. To study the thermal stability of DLC overcoating film, laser irradiation is often applied to heat up the DLC film on the multi-layered structure [7-8]. To fully understand the thermal instability of DLC film, it is of importance to investigate the laser induced temperature increase in the multi-layered structure with the DLC layer.

Mansuripur et al. [9] and Mansuripur and Connell [10] have developed an optical absorption model to predict local temperature increase in stationary and moving multi-layered media in magneto-optical recording, respectively. In the optical absorption model, the laser is regarded as an electromagnetic wave. The absorption rate of optical energy by the disk medium is derived from Maxwell equations, which is incorporated into the energy equation by a source term. Itagi [11] developed a finite volume method (FVM) in the reference frame attached to the moving heat source to solve the problems on laser heating in layered materials. To model laser heating in the multi-layered media of the hard disk driver, a heat flux model, which simplifies the heating process as a heat flux imposed at the disk surface, has been applied in the previous studies (e.g. [12, 13]). In this heat flux model, the absorptivity of the disk surface has to be determined empirically and the unsteady energy conservation equation can then be solved numerically.

As mentioned above, DLC is often applied as an overcoating layer on the multi-layered structure. This DLC layer is usually neglected in the numerical simulations on laser heating process because of the ultra-thin nature of the film [12, 13]. In the studies of the thermal instability of DLC film, information on the effect of the DLC layer thickness on local temperature increase is still lacking. However, the thermal conductivity of DLC is much lower than that of metal and the presence of the DLC layer may affect the absorption and reflection of laser energy. It would be important to quantitatively investigate the effect of the DLC layer on local temperature increase induced by laser heating.

In the following parts, we demonstrate how the DLC layer affects the laser energy absorption and, in consequence, the temperature distribution in the multi-layered structure. The optical absorption model is adopted in our simulations. The advantage of the optical absorption model is that the absorption rate can be determined from the materials' properties and the energy equation can then be solved numerically without any empirical parameters. It is worth mentioning that the laser heating duration in the present study is in the order of nanosecond. The traditional energy equation based on Fourier's law is thus applicable. However, for ultrashort laser pulse (femtosecond), the nonequilibrium energy transfer needs to be considered [14-17].

The outline of the paper is as follows. In the Numerical Method section a succinct description of the governing equations and boundary conditions for the energy conservation and numerical techniques for solving these equations are provided. This is followed by a presentation and discussion of the effect of the DLC layer on local temperature increase in the Results and Discussion section. And the concluding remarks are drawn in the last section.

Numerical Method

In the present study, we concern the effect of a thin DLC layer on local temperature increase induced by laser heating. This thin DLC layer is deposited on top of the multi-layered structure. A schematic of a typical multi-layered structure is shown in Figure 1. The structure consists of substrate, DLC and several other function layers. The application background for this type of structures is data storage industry. A laser beam with wave length λ and power P_W is shot onto the media. The laser beam may move against the media, which reflects the relative motion of the rotating disk and the laser. The propagation of the laser wave in the disk medium is governed by the following Maxwell equation:

$$\nabla^2 E_k(z) + \left(\frac{2\pi}{\lambda_0} N_k\right)^2 E_k(z) = 0 \quad (1)$$

$$\nabla \times E_k(z) - i\frac{2\pi}{\lambda_0} c_0 \xi H_k(z) = 0 \quad (2)$$

where $E_k(z)$ and $H_k(z)$ are electric and magnetic field components in the kth layer of disk structure (the layers are numbered from the bottom to the top), N_k is the complex refractive index ($N_k = Nr_k - iNe_k$), c_0 is the speed of light in vacuum, ξ is the magnetic permeability. Once the solutions of $E_k(z)$ and $H_k(z)$ are obtained, the rate of flow of energy through the multi-layered structure is calculated by invoking the Poynting vector theorem, which can be written as,

$$\begin{aligned} S_k(z) &= \mathrm{Re}\left[\frac{1}{2} E_k(z) H_k^*(z)\right] \\ &= \frac{1}{2c_0\xi}|A_k|^2 \left[Nr_k \left(e^{-\frac{4\pi Ne_k}{\lambda_0}\left(z-\sum_{j=k+1}^{n+1}\delta_j\right)} - |B_k|^2 e^{+\frac{4\pi Ne_k}{\lambda_0}\left(z-\sum_{j=k+1}^{n+1}\delta_j\right)} \right) \right. \\ &\quad \left. -2Ne_k |B_k| sin\left(\frac{4\pi Nr_k}{\lambda_0}\left(z - \sum_{j=k+1}^{n+1}\delta_j\right) + \Phi(B_k) \right) \right] \end{aligned} \quad (3)$$

where δ_k is the kth thickness layer, the coefficients A_k and B_k denote the light amplitude and the reflection in the kth layer, respectively. Note that the total number of layers (excluding the lubricant film) is n. The (n+1)th layer denotes the disk surface, which has zero thickness. A_k and B_k can be obtained in view of the continuity requirements at the boundaries when solving Eqs. (1) and (2), which can be expressed as [9],

$$B_k = \frac{\dfrac{N_k - N_{k+1}}{N_k + N_{k+1}} + B_{k-1}}{1 + \dfrac{N_k - N_{k+1}}{N_k + N_{k+1}} B_{k-1}} e^{-i\frac{4\pi N_k}{\lambda_0}\delta_k} \qquad 2 \le k \le n+1 \tag{4}$$

$$A_k = \frac{e^{-i\frac{2\pi N_{k+1}}{\lambda_0}\delta_{k+1}} + B_{k+1} e^{i\frac{2\pi N_{k+1}}{\lambda_0}\delta_{k+1}}}{1 + B_k} A_{k+1} \qquad 1 \le k \le n \tag{5}$$

$$B_1 = 0; \quad A_{n+1} = \sqrt{2c_0\mu} \tag{6}$$

If the laser intensity distribution in the x-y plane can be expressed by the Gaussian function, the local heat generation rate can then be written as

$$\dot{Q}_k = -\frac{P_W}{\pi r^2}\frac{dS_k}{dz} e^{-\frac{(x-x_0)^2+(y-y_0)^2}{r^2}} \tag{7}$$

where x_0 and y_0 are the spatial coordinates for the centre of the laser beam, which moves related to the rotating disk, and r is e^{-1} radius of the Gaussian beam. The unsteady heat conservation equation in the rotating frame can then be written as,

$$\frac{\partial T}{\partial t} = \alpha_k \left(\frac{\partial^2 T}{\partial x^2} + \frac{\partial^2 T}{\partial y^2} + \frac{\partial^2 T}{\partial z^2} \right) + \frac{\dot{Q}_k}{\rho_k C p_k} \tag{8}$$

where t is time, T is the temperature, α_k, ρ_k, Cp_k are the thermal diffusivity, the density, and the specific heat capacity of the kth layer medium, and x, y, z are the spatial coordinates. Here we only consider the motion of laser spot in the x-direction. If the center of the laser spot is initially located at the origin (0, 0) of the top surface, the variation of x_0 with time can be expressed as $x_0 = u_L \cdot t$, where u_L is the scanning speed of laser. The zero speed of the laser ($u_L = 0$) means stationary heating.

A finite volume method with the second order accuracy in both time and space is used to solve the governing equations [18, 19]. For the purpose of validation, we simulate the laser induced heating during the thermomagnetic writing on a magnetooptic disk [9]. The magnetooptic disk consists of five layers, i.e. 1) 100 nm glass, 2) 12 nm MnBi, 3) 72nm glass, 4) 32 nm aluminum, and 5) PMMA (infinite thickness compared with other layers). The thermal and optical properties of the above materials can be found in Mansuripur et al. [9]. The laser power turns on for 60 ns, the peak power is 2 mW, and the total energy is 96 pJ. The laser beam has wavelength of 632.8 nm and radius r = 350 nm. Heat convection from the surface is neglected. Figure 2 compares temperature increase along the z direction at the centre of laser beam between the present simulations and those of Mansuripur et al. [9]. The two results generally agree with each other. The discrepancy may be due to the simplifications in the numerical method made by Mansuripur et al. [9].

To further validate the present method, a comparison is made between the results obtained by the present FVM code and the commercial software ANSYS. In this comparison, the multi-layered structure shown in Figure 1 is applied. The DLC layer thickness is 4 nm. The parameters related to the laser beam are: the radius r = 70 nm, the scanning velocity u_x = 10 m/s, the wavelength λ = 632.8 nm, the power P_W = 2 mW. The thermal and optical properties of the materials are summarized in Table 1. The centre of laser beam is initially located at the centre of simulation domain (0, 0, 0). Figure 3 shows the instantaneous temperature profile along the horizontal line on the top surface at t = 2.5 ns and 20 ns. The good agreement between the two simulations confirms the validation of the present method.

Results and Discussion

In the present study, the thickness of each layer of the multi-layered structure is fixed except that of the DLC layer. Figure 4 presents the laser energy flow rate along the *z* direction in the multi-layered structure. The arrows in the figure indicate the interface between two adjacent layers. We only show the energy flow rate up to the depth of $z = 100$ nm because it approaches zero when $z > 100$ nm. Figure 4 indicates that the energy transmitted into the multi-layered structure increases if the DLC layer is present and the thicker the DLC layer, the more the energy is transferred into the structure. For example, the total laser energy transferred into the disk is 37.3%, 40.2%, 48.3%, and 67.2% for the cases of 0 nm, 4 nm, 12 nm, and 25 nm DLC layers, respectively. However, most of this increased part of the total energy is absorbed by the DLC layer. The energy absorbed by the other layers underneath the DLC layer does not change significantly with the variation of the thickness of DLC layer. The absorption rates of FePt layer are 20.1%, 20.6%, 21.9%, and 22.6% for the cases of 0 nm, 4 nm, 12 nm, and 25 nm DLC layers, respectively.

Figure 5 shows the distributions of temperature increase (ΔT) in the middle *x*-*z* plane at $t = 40$ ns for the cases of 0 nm, 4 nm, and 12 nm DLC layers. The arrows indicate the boundaries between different layers. The laser power and the relative scanning velocity are 15 mW and 10 m/s, respectively. The laser is turned on for 40 ns and then turned off. The ΔT level is much higher for the case of 12 nm DLC layer than those of 0 nm and 4 nm DLC layers. The trends of temperature distribution are generally similar for all the three cases except that the temperature gradient is larger in the 12 nm DLC layer (Figure 5c). The larger temperature gradient is due to lower thermal conductivity of DLC. However, for the thin DLC layer (Figure 4b), the temperature gradient in the *z* direction in the DLC layer is negligible.

Figure 6 records the time history of the maximum temperature increase (ΔT_{max}) in the multi-layered structure. Immediately after the laser is turned on, ΔT_{max} increases rapidly with time and then increases slowly when t > ~5 ns. ΔT_{max} increases more rapidly at the initially stage when the DLC layer is present, especially for a thicker DLC layer. The temperature differences among different disk structures (different DLC thickness) also increase with the elapse of time but the increase speed gradually approaches zero with increasing t. After the laser is turned off, the temperature decays sharply.

Figure 7a compares ΔT profiles along the horizontal center line of the top surface at t = 40 ns for different DLC thickness. Without the DLC layer, the maximum ΔT is around 210 K. With 4 nm DLC layer, the maximum ΔT increases to about 230K. When the thickness of DLC layer increases to 12 nm, the maximum ΔT rapidly increases to about 310K, about 100K higher than that without the DLC layer. The maximum ΔT reaches 640K when the thickness of DLC layer is 25nm. Figure 7a also shows that the peak region of temperature profile and the temperature gradient in the horizontal direction increase with increasing DLC thickness.

Figure 7b shows ΔT profiles along the z direction at the center of the laser spot at t = 40 ns for different DLC thickness. The temperature gradient in the layers from FePt to Ta is small for all the four cases shown in Figure 7b. The thermal conductivities of materials in these layers are much larger than that of substrate (glass), thus resulting in smaller temperature gradient. The temperature gradients in 12 nm and 25nm DLC layers are rather large. However, the temperature gradient in 4 nm DLC layer is negligibly small because of the ultra-thin nature of the layer. The comparison of temperature gradient in the DLC layers with different thickness indicates that the temperature increase ΔT is higher and the temperature gradient is larger in the thicker

DLC layer. The temperature increase ΔT in the structure with the thicker DLC layer is higher than that in the structure with the thinner DLC layer. This temperature different is more prominent in the DLC layer than that in other layers.

The above results indicate that the presence of the DLC layer causes an increase in ΔT in the multi-layered structure induced by laser heating although the increase is marginal for an ultrathin DLC layer (e.g. 4 nm). As shown in Figure 4, the presence of the DLC layer increases the laser energy flow rate. This means that more energy is absorbed by the disk, thus leading to a higher temperature. More important, most of this increased part of the total energy is absorbed by the DLC layer. When the DLC layer is thicker, the laser energy absorbed by it is more significant. Moreover, DLC has a very low thermal conductivity of $O(1)$ W/(mK). The heat accumulates in the DLC layer due to its low thermal conductivity, which results in a significant increase in ΔT when the DLC layer is thick. The thermal diffusivity of DLC is about two-order lower than those of FePt and CrRu. This means the heat transfer rate in the DLC layer is about 100 times slower than those in the FePt and CrRu layers, which causes a higher temperature and a larger temperature gradient in the DLC layer.

Wu [20] also reported the temperature field on the disk subject to laser heating. His results [20] indicate that, to achieve about the same temperature increase, the laser power used for a glass substrate is about 100 times stronger than that for an aluminum substrate if the laser absorptivity for both substrates are the same. It is known that the thermal diffusivity of aluminum is about 100 times larger than that of glass. Thus, when the energy absorbed by the DLC layer is comparable to that absorbed by other layers, the final temperature increase is largely determined by the DLC layer due to its low thermal diffusivity. However, for 4 nm DLC layer, the energy absorbed by it is less than 2%. The other layers thus have a decisive effect on ΔT in the disk. Besides this, the ultra-thin nature results in a uniform temperature distribution along the *z* depth in the DLC layer.

In the above analysis, the laser scanning velocity is fixed at 10 m/s. This velocity may vary at different situations. A parametric study is thus conducted to demonstrate its effect. Figure 8 presents ΔT profiles along the *z* direction at the center of the laser spot at t = 40 ns for different u_L. The data are only shown for two DLC thicknesses. The vertical dash lines in Figure 8 indicate the interface between the DLC and FePt layers. The results indicate that when u_L = 10 m/s, the laser scanning velocity has a small effect on the temperature profiles (compared with those for u_L = 0). However, when u_L = 50 m/s, its effect becomes significant. Compared with those for u_L = 0, the maximum surface temperature at u_L = 50 m/s decreases by about 50 K and 100 K for 4 nm and 25 nm DLC layers, respectively. Our simulations show that when the scanning velocity is faster than 30 m/s, the temperature drop in the multi-layered structure becomes significant. And the thicker the DLC layer is, the more pronounced the temperature drop is. Figure 8 also shows that the temperature difference at the same location for different laser scanning velocity is almost constant in the layers between the DLC and the substrate. The layers are metal-like materials and thus have high thermal conductivities. The thermal diffusion speed is thus faster than the laser scanning velocity, which results in a uniform temperature different along the *z* direction in these layers. However, in the substrate layer (glass), the temperature difference at the same location for different laser scanning velocity increases with increasing depth, which is due to low thermal conductivity of glass.

Figure 9 summarizes the maximum temperature increase ΔT_{max} in the top surface and the FePt layer at different DLC thickness and laser scanning velocity. For the same u_L, both the ΔT_{max} in the top surface and the FePt layer increase with increasing DLC thickness. The increase rate for the ΔT_{max} in the top surface is faster than that for the ΔT_{max} in the FePt layer. The difference between ΔT_{max} at different velocities for the same location (comparing curves with the same symbols) slightly increases with increasing DLC thickness.

The above results indicate that the DLC layer with its thickness more than 4 nm has significant effect on ΔT in the disk. This effect mainly results from the energy absorbed by the DLC layer. To further demonstrate this aspect, a numerical experiment is conducted by artificially setting the extinction index of DLC to be zero. In this situation, the energy absorbed by the DLC layer is zero. We shall refer this numerical experiment as the zero absorption case for simplification.

Figure 10a shows the laser energy flow rate along the z direction for the zero absorption case. For a thicker DLC layer, more laser energy is transmitted into the multi-layered structure. For the same DLC thickness, the total energy transmitted into the multi-layered structure for the zero absorption case is less than that for the nonzero absorption case (Comparing Figure 10a with Figure 4). However, the energy transmitted into the FePt layer for the zero absorption case is more than that for the nonzero absorption case (Comparing Figure 10a with Figure 4). For the zero absorption case, the absorption rates in the FePt layer are 21.3%, 24.3%, and 31.9% for the cases of 4 nm, 12 nm, and 25 nm DLC layers, respectively. It is worth mentioning that the increase in absorption rate in the FePt layer is rather significant for 25 nm DLC layers.

The corresponding temperature profiles along the z direction at the centre of the laser spot at t = 40 ns are presented in Figure 10b. The laser power and the relative scanning velocity are 15 mW and 10 m/s, respectively. As expected, the temperature is higher if the DLC layer is thicker (due to higher absorption rate in the FePt Layer). The maximum ΔT is around 220 K, 250K, and 310K for the case of 4 nm, 12 nm, and 25 nm

DLC layers, respectively. The temperature gradient along the *z* direction in the DLC layer is almost zero. For the thickest case of 25 nm DLC layer, the temperature slightly decreases along the negative *z* direction.

Figure 11 compares the maximum temperature increase ΔT_{max} in the FePt layer of the multi-layered structure with different DLC thicknesses for zero and nonzero absorption in the DLC layer. The ΔT_{max} in the FePt layer for the nonzero absorption case is always higher than that for zero absorption case with the same DLC thickness. The temperature difference between the zero and nonzero absorption cases grows rapidly with increasing DLC thickness.

The comparison between Figure 4 and Figure 10b indicates that the energy absorbed by the FePt layer for the zero absorption case is more than that for the nonzero absorption case with the same DLC thickness. However, the temperature increases in the FePt layer shows opposite trend. This further confirms that the energy absorbed by the DLC layer is the main contribution of additional temperature increase compared with the zero DLC thickness case. This energy accumulates in the DLC layer due to its low thermal conductivity, which results in significant local temperature increase.

Conclusion

In the present study, transient heat transfer in the multi-layered structure subject to laser heating is simulated by a finite volume code. The laser absorption rate in the multi-layered structure is derived from Maxwell equations, which is solely determined from the materials' properties. The absorption rate is incorporated into the energy equation by a source term and the energy equation is then solved numerically without any empirical parameters.

The effect of the thickness of the DLC layer on local temperature increase is discussed. Compared with that in the structure without the DLC layer, the presence of the DLC layer on the top of multi-layered structure enhances local temperature increase. This enhancement grows rapidly with an increase in the thickness of the DLC layer. The temperature gradient along the depth direction in the DLC layer increases with increasing DLC thickness. Thus, the temperature difference between the DLC layer and its underneath layer becomes larger when the DLC layer is thicker. The scanning velocity of the laser beam on local temperature increase is investigated. When the scanning velocity exceeds 30 m/s, the temperature drop in the multi-layered structure becomes significant. And the thicker the DLC layer is, the more pronounced the temperature drop is.

The presence of the DLC layer increases the laser energy flow rate in the multi-layered structure. This indicates that more energy is absorbed by the disk, thus leading to a higher temperature. More importantly, most of this increased part of the total energy is absorbed by the DLC layer. Because DLC has a very low thermal conductivity, the heat accumulates in the DLC layer. Significant temperature increase in the DLC layer occurs when it is thick. The numerical experiment also confirms that this aspect is the main contribution of the additional temperature increase compared with that in the multi-layered structure without the DLC layer. The present study provides important information on the thermal design of the overcoating layer for the multi-layered structure subject to laser heating.

References

[1] C. Casiraghi, J. Robertson, and A. C. Ferrari, Diamond-like carbon for data and beer storage, Mater. Today, vol. 10, pp. 44-53, 2007.

[2] M. Hakovirta, J. E. Vuorinen, X. M. He, M. Nastasi, and R. B. Schwarz, Heat capacity of hydrogenated diamond-like carbon films, Appl. Phys. Lett., vol. 77, pp. 2340, 2000.

[3] M. Shamsa, W. L. Liu, A. A. Balandin, C. Casiraghi, W. I. Milne, and A. C. Ferrari, Thermal conductivity of diamond-like carbon films, Appl. Phys. Lett., vol. 89, pp. 161921, 2006.

[4] J. K. Luo, A. J. Flewitt, S. M. Spearing, N. A. Fleck, and W. I. Milne, Normally closed microgrippers using a highly stressed diamond-like carbon and Ni bimorph structure, Appl. Phys. Lett., vol. 85, pp. 5748, 2004.

[5] M. H. Kryder, E. C. Gage, T. W. McDaniel, W. A. Challener, R. E. Rottmayer, G. Ju, Y. T. Hsia, and M. F. Erden, Heat Assisted Magnetic Recording, Proceedings of the IEEE, vol. 96, pp. 1810-1835, 2008.

[6] T. Sameshima, and N. Andoh, Heating layer of diamond-like carbon films used for crystallization of silicon films, Jpn. J. Appl. Phys., vol. 44, pp. 7305-7308, 2005.

[7] R. Kalish, Y. Lifshitz, K. Nugent, and S. Prawer, Thermal stability and relaxation in diamond-like-carbon. A Raman study of films with different sp3 fractions (ta-C to a-C), Appl. Phys. Lett., vol. 74, pp. 2936, 1999.

[8] N. Wang and K. Komvopoulos, Thermal stability of ultrathin amorphous carbon films for energy-assisted magnetic recording, IEEE Trans. Magn., vol. 47, pp. 2277-2282, 2011.

[9] M. Mansuripur, G. A. N. Connell, and J. W. Goodman, Laser-induced local heating of multilayers, Appl. Optics, vol. 21, pp. 1106-1114, 1982.

[10] M. Mansuripur, and G. A. N. Connell, Laser-induced local heating of moving multilayer media, Appl. Optics, vol. 22, pp. 666-670. 1983.

[11] A. V. Itagi, Finite volume method for the Fourier heat conduction in layered media with a moving volume heat source, Jpn. J. Appl. Phys., vol. 46, pp. 1482-1489, 2007.

[12] L. Wu and F. E. Talke, Modeling laser induced lubricant depletion in heat-assisted-magnetic recording systems using a multiple-layered disk structure, Microsys. Technol., vol. 17, pp. 1109-1114, 2011.

[13] Y. Zeng, W. D. Zhou, X. Huang, and S. K. Yu, Numerical study on thermal-induced lubricant depletion in laser heat-assisted magnetic recording systems, International Journal of Heat and Mass Transfer, vol. 55, pp. 886-896, 2012.

[14] B. S. Yilbas, Laser short-pulse heating of a gold surface: comparison of absorption and surface heat flux heating, Num. Heat Trans. A, vol. 52, pp. 87-100, 2007.

[15] J. K. Chen, J. E. Beraun and C. L. Tham, Investigation of thermal response caused by pulse laser heating, Num. Heat Trans. A, vol. 44, pp. 705-722, 2003.

[16] M. Iwamoto, M. Ye, C. P. Grigoropoulos and R. Greif, Numerical analysis of pulsed laser heating for the deformation of metals, Num. Heat Trans. A, vol. 34, pp. 791-804, 1998.

[17] I. Z. Naqavi and B. S. Yilbas, Laser nanosecond pulse heating of surfaces and thermal stresses, Num. Heat Trans. A, vol. 40, pp. 295-316, 2001.

[18] P. Yu, W. D. Zhou, S. K. Yu and K. S. Myo, Modeling laser heated thin film media for heat assisted magnetic recording, Microsys. Technol., accepted.

[19] P. Yu, W. D. Zhou, S. K. Yu and Y. Zeng, Laser-induced local heating and lubricant depletion in heat assisted magnetic recording systems, Int. J. Heat Mass Trans. vol. 59, pp. 36-45, 2013.

[20] L. Wu, Modelling and simulation of the lubricant depletion process induced by laser heating in heat-assisted magnetic recording system, Nanotechnology, vol. 18, p. 215702, 2007.

List of Tables

List of Figures

Table 1 Material properties for the multi-layered structure

	DLC	FePt	TiN	CrRu	Ta	Glass
order	6	5	4	3	2	1
density (kg/m^3)	2300	15000	5400	9686	16600	2440
specific heat (J/[kg K])	1000	200	600	341	140	830
thermal conductivity (W/[mK])	1.00	75.0	19.0	96.0	57.0	1.14
refractive index	2.17-0.46i	2.65-3.48i	1.35-2.76i	3.69-4.79i	2.70-2.16i	1.56
thickness (nm)	-	12	10	60	3	infinite

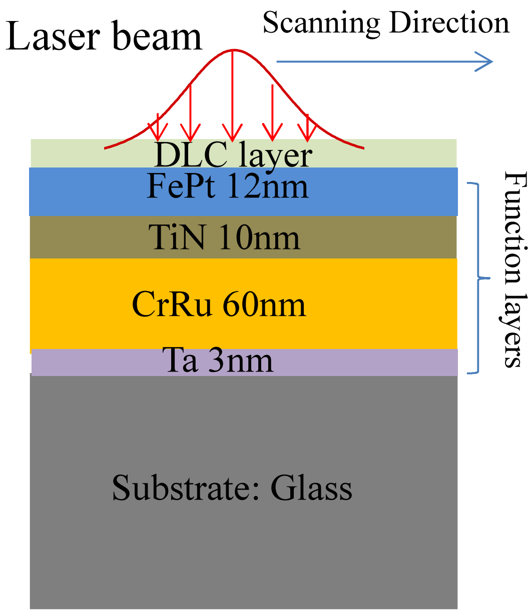

Figure 1 Sketch of multi-layered structure.

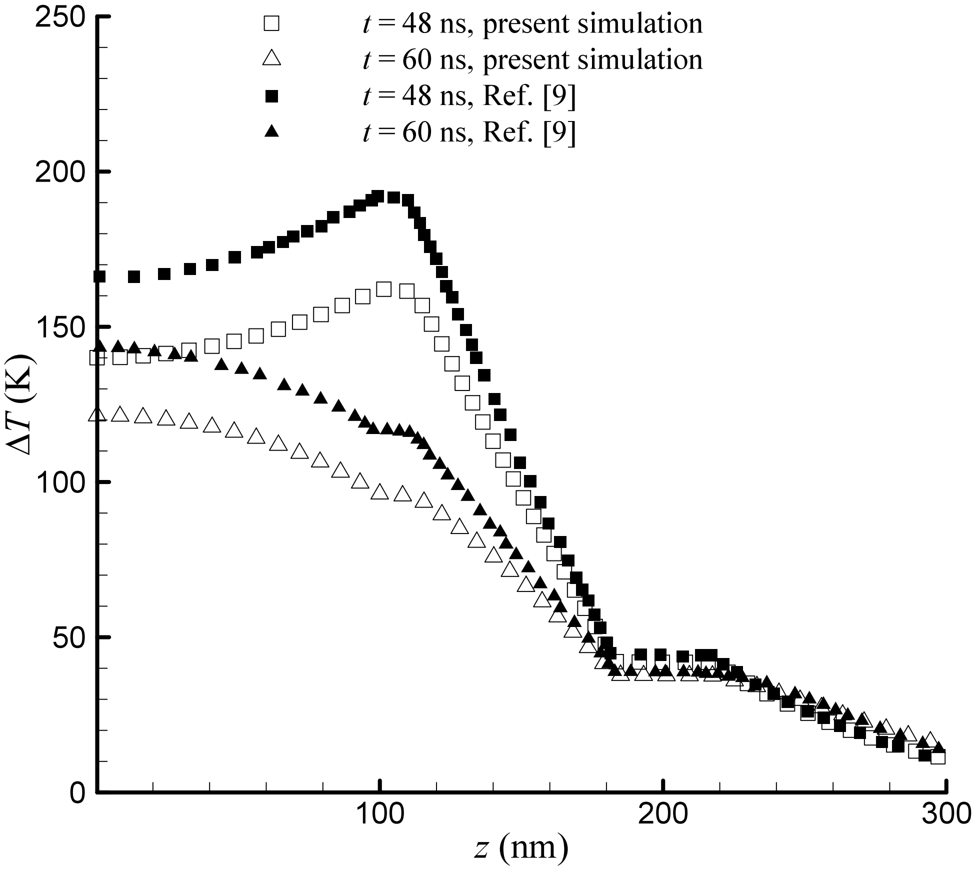

Figure 2 Temperature increase along the *z* direction at the centre of laser beam for laser induced heating during the thermomagnetic writing on a magnetooptic disk.

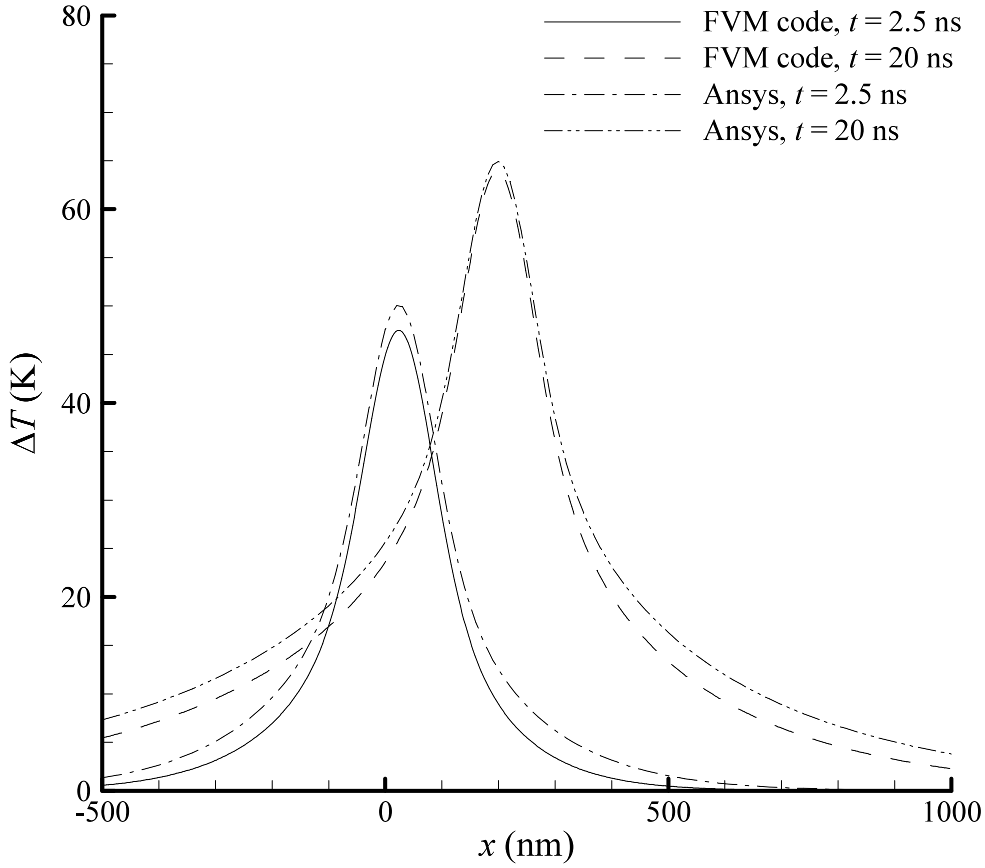

Figure 3 Horizontal surface temperature increase profile for laser induced heating in the multi-layered structure.

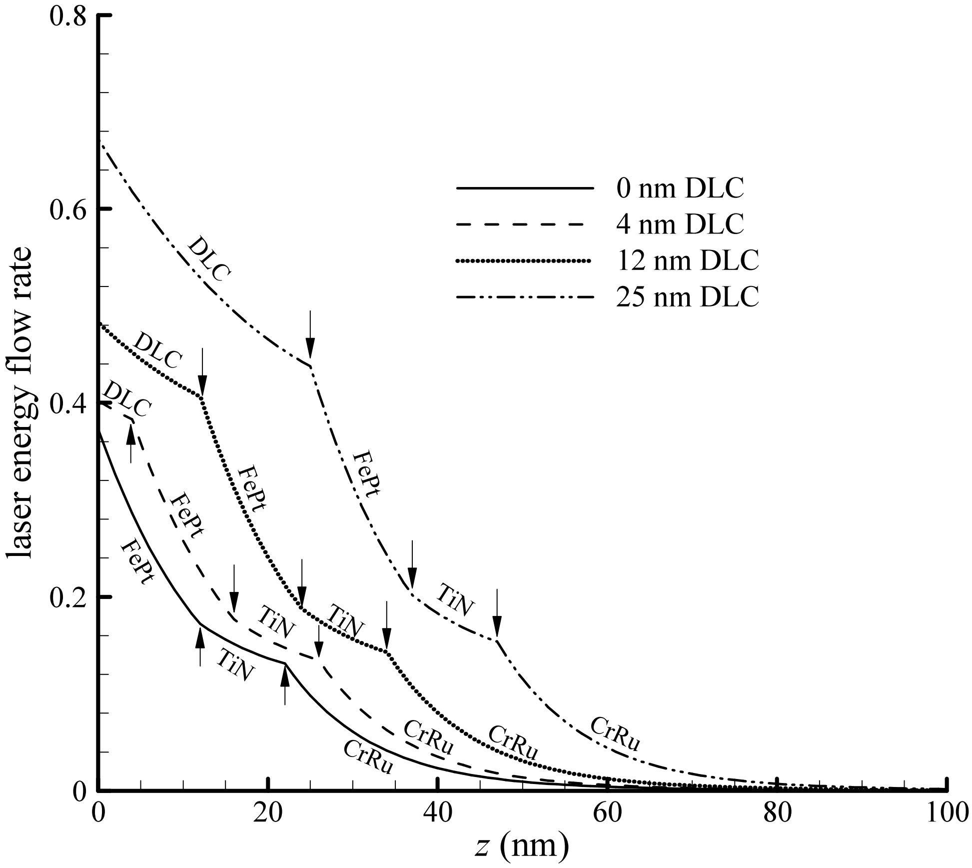

Figure 4 Laser energy flow rate along the z direction in the multi-layered structure for different DLC thickness.

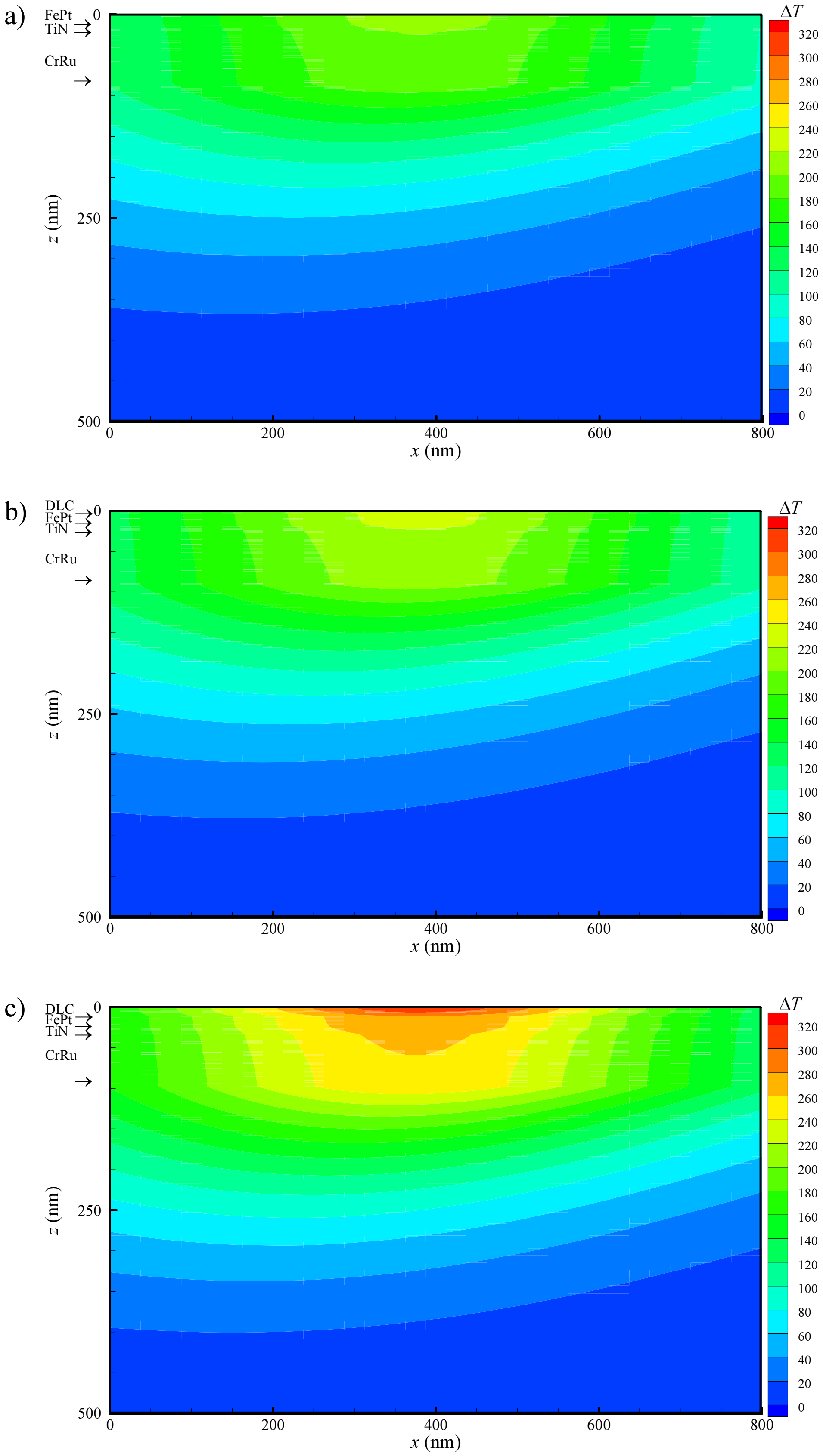

Figure 5 Distributions of temperature increase (ΔT) in the middle x-z plane at t = 40 ns, a) without the DLC layer, b) 4 nm DLC layer, c) 12 nm DLC layer. The arrows indicate the boundaries between different layers.

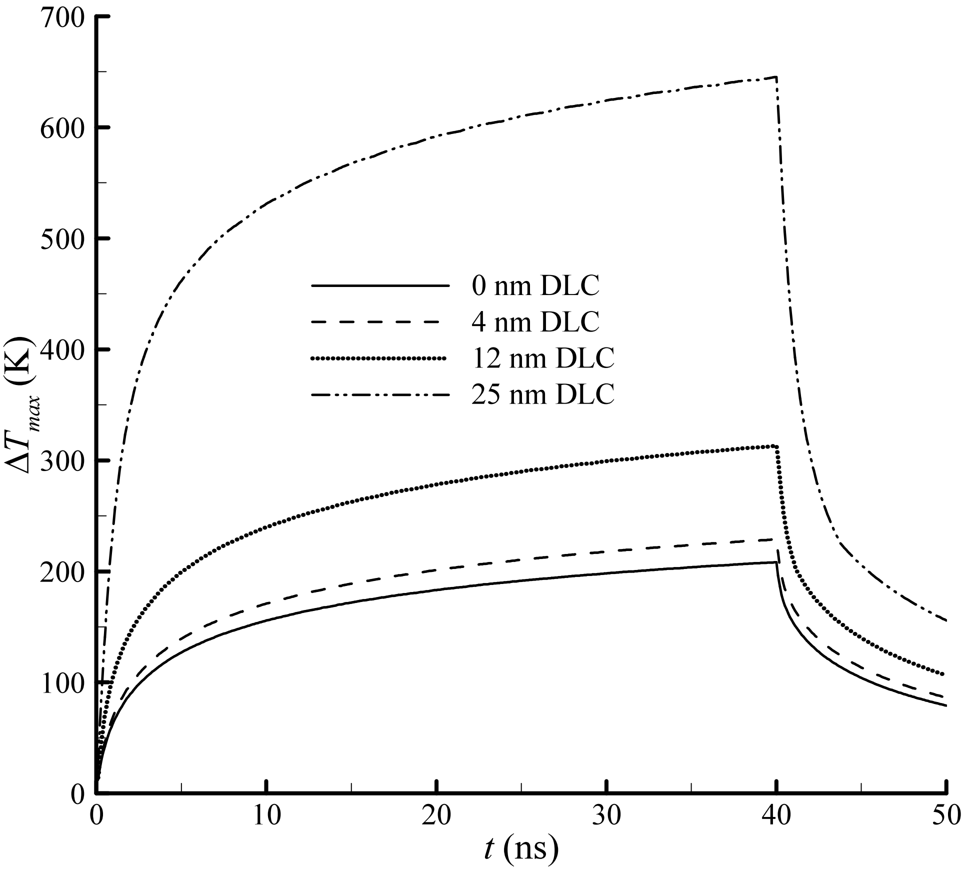

Figure 6 Time history of maximum temperature increase in the multi-layered structure.

a)

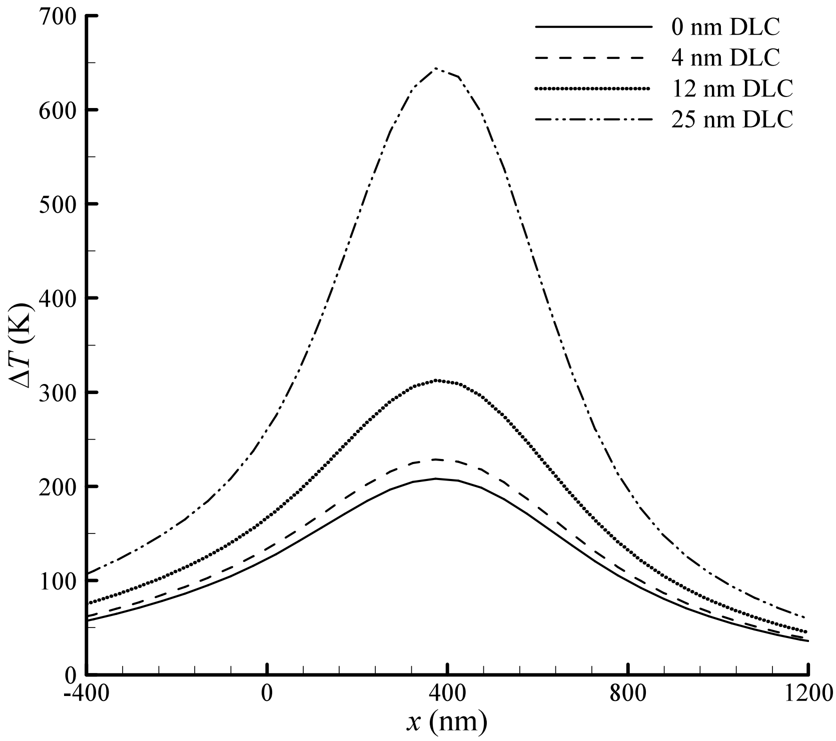

b)

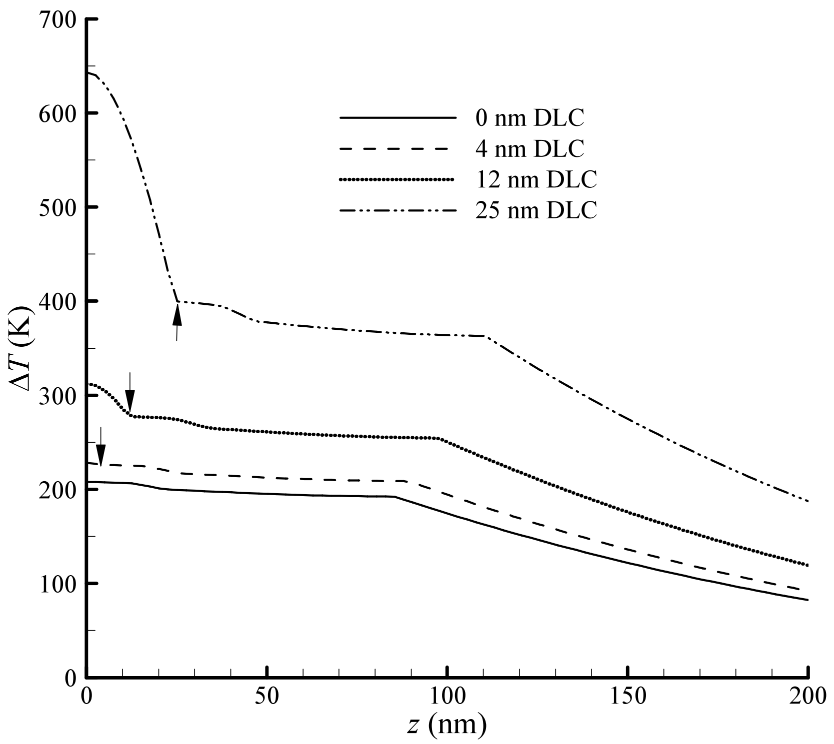

Figure 7 Temperature increase profiles at t = 40 ns for the different structures, a) along the horizontal center line of top surface, and b) along the z direction at the centre of laser beam.

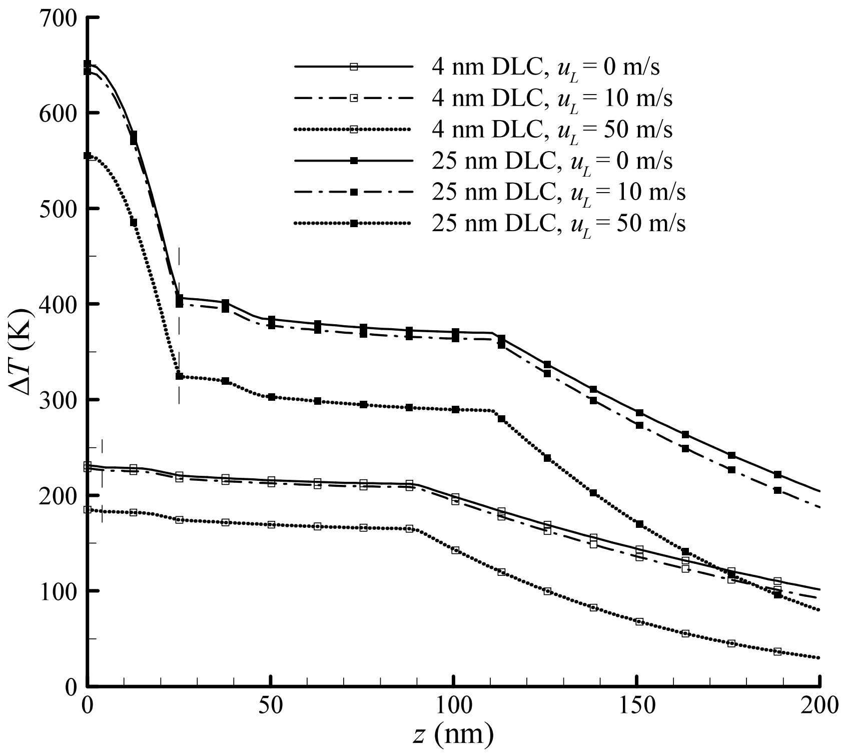

Figure 8 Effect of laser scanning velocity on the temperature increase profile along the z direction at the centre of laser beam at t = 40 ns.

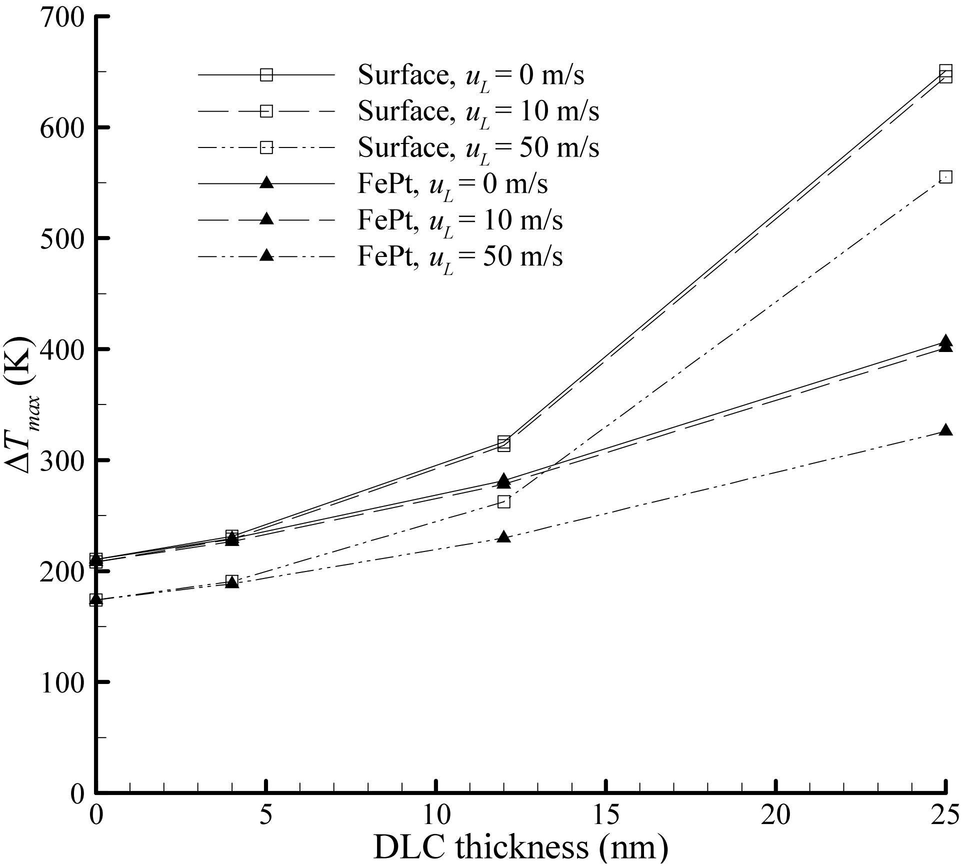

Figure 9 Maximum temperature increase on the surface and the FePt layer at different DLC thicknesses and laser scanning velocities.

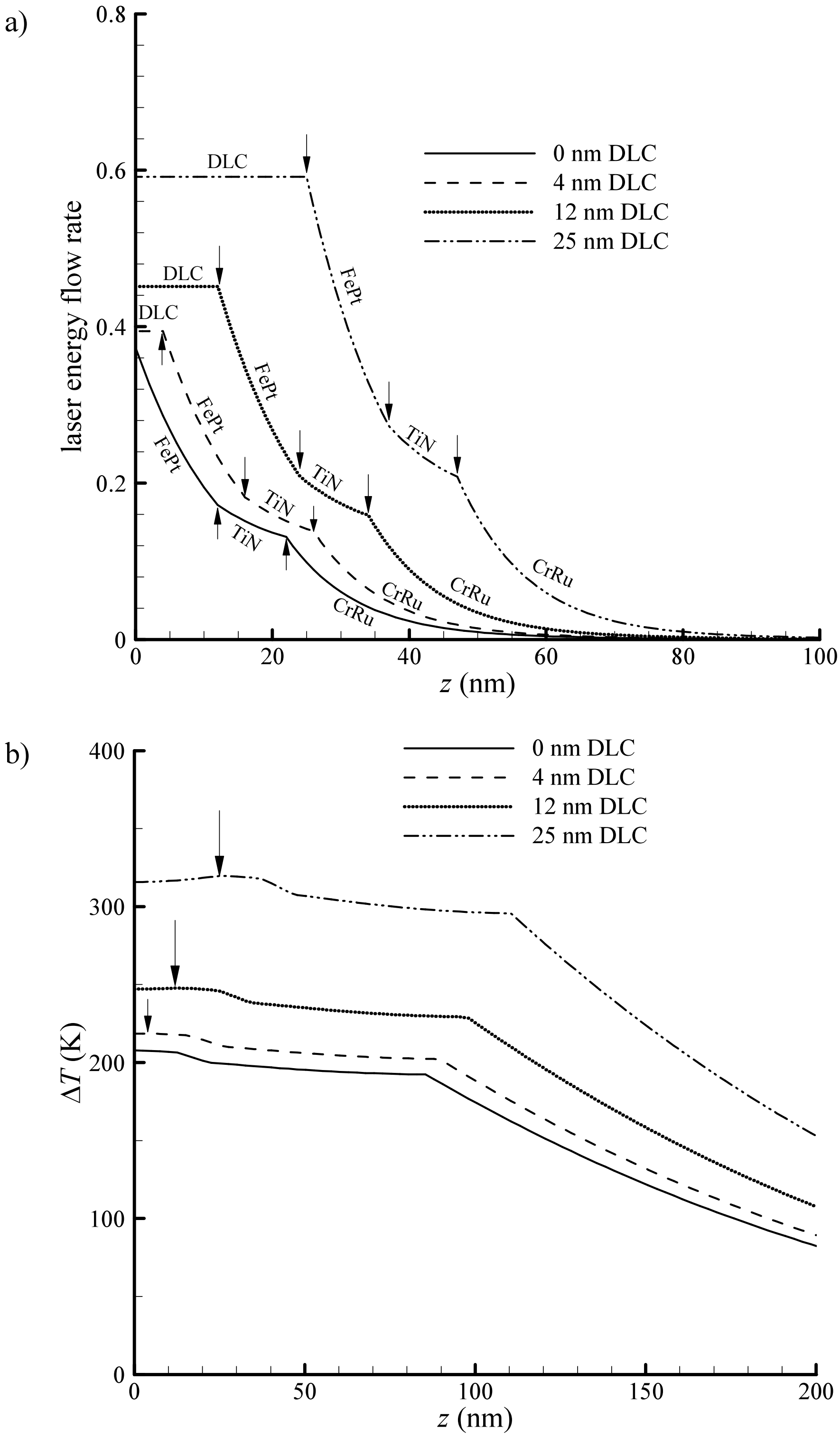

Figure 10 a) Laser energy flow rate along the z direction in the multi-layered structure, and b) Temperature increase profiles along the *z* direction at the centre of laser beam at *t* = 40 ns. The extinction coefficient *Ne* of DLC is set to zero.

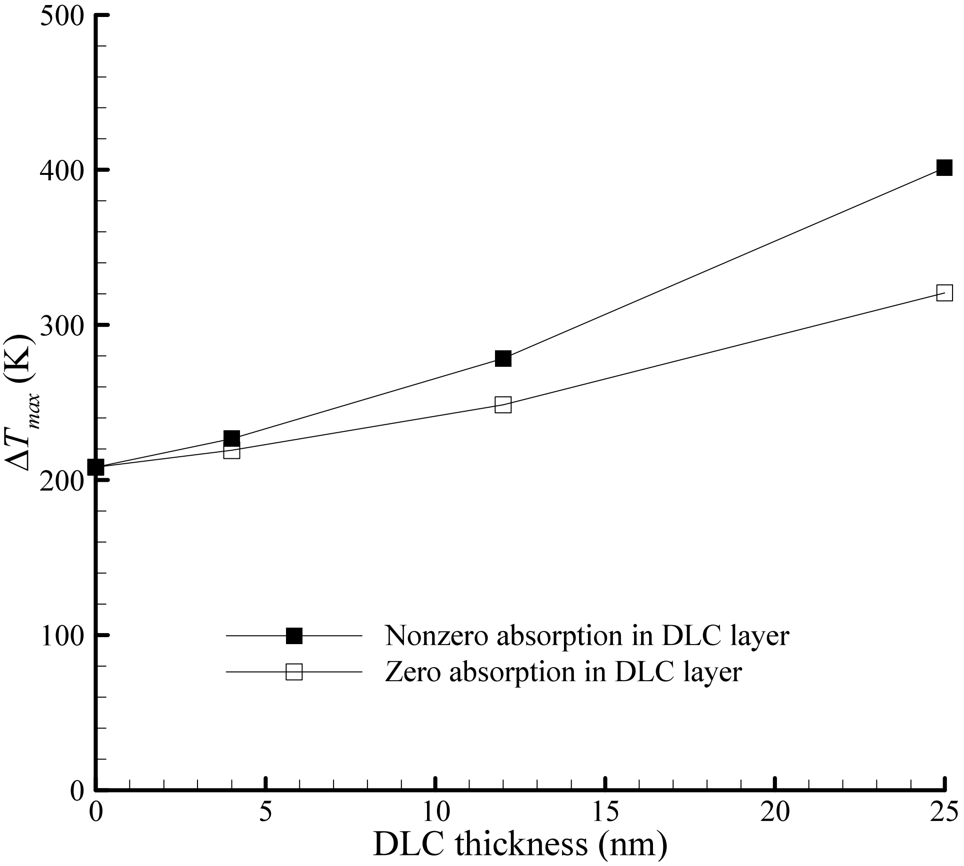

Figure 11 Comparison of the maximum temperature increase in the FePt Layer of the multi-layered structure with different DLC thicknesses for zero and nonzero absorption in the DLC layer.